Dissolved gases in hydrothermal (phreatic) and geyser eruptions at Yellowstone National Park, USA

Shaul Hurwitz[1], Laura E. Clor[1], R. Blaine McCleskey[2], D. Kirk Nordstrom[2], Andrew G. Hunt[3], and William C. Evans[1]
[1]U.S. Geological Survey, Menlo Park, California 94025, USA
[2]U.S. Geological Survey, Boulder, Colorado 80303, USA
[3]U.S. Geological Survey, Denver, Colorado 80225, USA

ABSTRACT

Multiphase and multicomponent fluid flow in the shallow continental crust plays a significant role in a variety of processes over a broad range of temperatures and pressures. The presence of dissolved gases in aqueous fluids reduces the liquid stability field toward lower temperatures and enhances the explosivity potential with respect to pure water. Therefore, in areas where magma is actively degassing into a hydrothermal system, gas-rich aqueous fluids can exert a major control on geothermal energy production, can be propellants in hazardous hydrothermal (phreatic) eruptions, and can modulate the dynamics of geyser eruptions. We collected pressurized samples of thermal water that preserved dissolved gases in conjunction with precise temperature measurements with depth in research well Y-7 (maximum depth of 70.1 m; casing to 31 m) and five thermal pools (maximum depth of 11.3 m) in the Upper Geyser Basin of Yellowstone National Park, USA. Based on the dissolved gas concentrations, we demonstrate that CO_2 mainly derived from magma and N_2 from air-saturated meteoric water reduce the near-surface saturation temperature, consistent with some previous observations in geyser conduits. Thermodynamic calculations suggest that the dissolved CO_2 and N_2 modulate the dynamics of geyser eruptions and are likely triggers of hydrothermal eruptions when recharged into shallow reservoirs at high concentrations. Therefore, monitoring changes in gas emission rate and composition in areas with neutral and alkaline chlorine thermal features could provide important information on the natural resources (geysers) and hazards (eruptions) in these areas.

INTRODUCTION

Nearly half of the world's geysers and many of the largest hydrothermal explosion craters on Earth are in Yellowstone National Park (Wyoming, USA), predominantly in areas where water temperatures approach boiling in the shallow subsurface (Fournier, 1989; Hurwitz et al., 2012; Hurwitz and Lowenstern, 2014). Geyser and hydrothermal eruptions exhibit a wide range of eruptive styles that are driven by the conversion of thermal energy into kinetic energy via vapor generation and expansion (Kieffer, 1989; Mastin, 1995; Thiéry and Mercury, 2009). However, whereas geysers episodically discharge liquid water, steam, and other gases into the atmosphere, hydrothermal eruptions (synonymous with hydrothermal explosions and phreatic eruptions) are discrete events that occur when pressures are sufficient to fracture the host rock, resulting in the ejection of steam, water, gas, and rock (Muffler et al., 1971; Browne and Lawless, 2001; Morgan et al., 2009). These eruptions are among the most frequent hazards in Yellowstone (Christiansen et al., 2007).

With the exception of a few studies limited in scope (Kennedy et al., 1988; Ladd, 2014), hypotheses suggesting that dissolved gases exert a significant control on hydrothermal and geyser eruptions were not supported by measurements (e.g., White, 1967; Hutchinson et al., 1997; Browne and Lawless, 2001; Lu and Kieffer, 2009). Further, measurements following research drilling in Yellowstone's geyser basins in the 1960s showed that temperature in the wells was below water vapor saturation (White et al., 1975), possibly resulting from gases dissolved in the thermal water. To test these hypotheses, in April 2015 we collected pressurized samples of thermal water that preserved dissolved gases in conjunction with precise temperature measurements with depth.

METHODS

Because collecting subsurface samples from the geysers themselves (such as Old Faithful Geyser) is impractical, we focused on the 74-m-deep research well Y-7 and on five thermal pools in Yellowstone's Upper Geyser Basin (Fig. 1A; Table 1; Table DR1 in the GSA Data Repository[1]). Pools were selected based on their accessibility, surface area, depth, and geographic position within the geyser basin. In well Y-7, samples were collected from three depths (maximum of 70.1 m), and at each pool, samples were obtained from the bottom (maximum of 11.3 m) and just below the water surface (Table 1). All of the pools have visible vents at the bottom through which bubbles episodically discharge; sample collection and temperature measurement were performed as close to the vents as possible.

Water temperature measurements were made with a precise pre-calibrated portable RTD logging system. Temperature measurements in well Y-7 were made between 1 m below the ground surface and near the bottom of the well at a depth of 73 m, at increments of 2–3 m (Fig. 1B). In each thermal pool, temperature was measured below the water surface and at the bottom, with varying intervals (Fig. 1C). Reported temperatures represent averages over 2 min at 5 s

[1]GSA Data Repository item 2016071, details and schematic of the sampling method, thermal pool locations, water chemistry, dissolved gas concentrations, noble gas isotope ratios, and temperature-dependent Henry's law constants, is available online at www.geosociety.org/pubs/ft2016.htm, or on request from editing@geosociety.org or Documents Secretary, GSA, P.O. Box 9140, Boulder, CO 80301, USA.

TABLE 1: CONCENTRATIONS AND PARTIAL PRESSURES OF DISSOLVED GASES, UPPER GEYSER BASIN, YELLOWSTONE NATIONAL PARK, USA

Sample	Site	Area (m^2)	Depth (m)	T (°C)	CO_2 (μmol/kg)	N_2 (μmol/kg)	CH_4 (μmol/kg)	O_2 (μmol/kg)	P_{CO_2} (kPa)	P_{N_2} (kPa)	P_{H_2O}* (kPa)
YNP15-01†	Well Y-7	0.01	13.7	82	2821	291	15.8	13.9	22	65	51
YNP15-03	Well Y-7		70.1	136	3365	159	14.7	5.5	36§	29	322
YNP15-04	Well Y-7		50.9	124	3231	146	12.7	5.4	34	29	225
YNP15-05	Black Sand Pool	490	6.1	94	20	89	1.0	8.3	0	20	82
YNP15-06	Black Sand Pool		1.5	93	14	80	0.7	12.9	0	18	79
YNP15-07	Punchbowl Spring	20	4.4	93	1033	48	1.3	12.6	9	11	79
YNP15-08	Punchbowl Spring		1.4	92	839	39	1.0	9.3	7	9	76
YNP15-09	Crested Pool	110	11.3	112	3	2	0.0	0.5	0	0	153
YNP15-10	Crested Pool		6.7	95	2	83	0.1	1.7	0	18	85
YNP15-11	Crested Pool		3.0	92	2	94	0.1	17.1	0	21	76
YNP15-12	East Chinaman Spring	1	5.0	95	198	78	0.7	0.2	2	17	85
YNP15-13	East Chinaman Spring		1.5	95	134	65	0.8	0.1	1	14	85
YNP15-14	Chinese Spring	1	4.6	97	111	51	0.3	0.2	1	11	90

Note: T—temperature; *P*—partial pressure.
*H_2O vapor pressure from National Institute of Standards and Technology database (htt-p://webbook.nist.gov/chemistry/fluid/).
†Sample is contaminated with air as indicated by high concentrations of air-derived gases.
§Calculated P_{CO_2} using the chemical speciation code SOLMINEQ.88 (Kharaka et al., 1988) is 42 kPa.

GEOLOGY, March 2016; v. 44; no. 3; p. 235–238 | Data Repository item 2016071 | doi:10.1130/G37478.1 | Published online 5 February 2016
© 2016 Geological Society of America. For permission to copy, contact editing@geosociety.org.

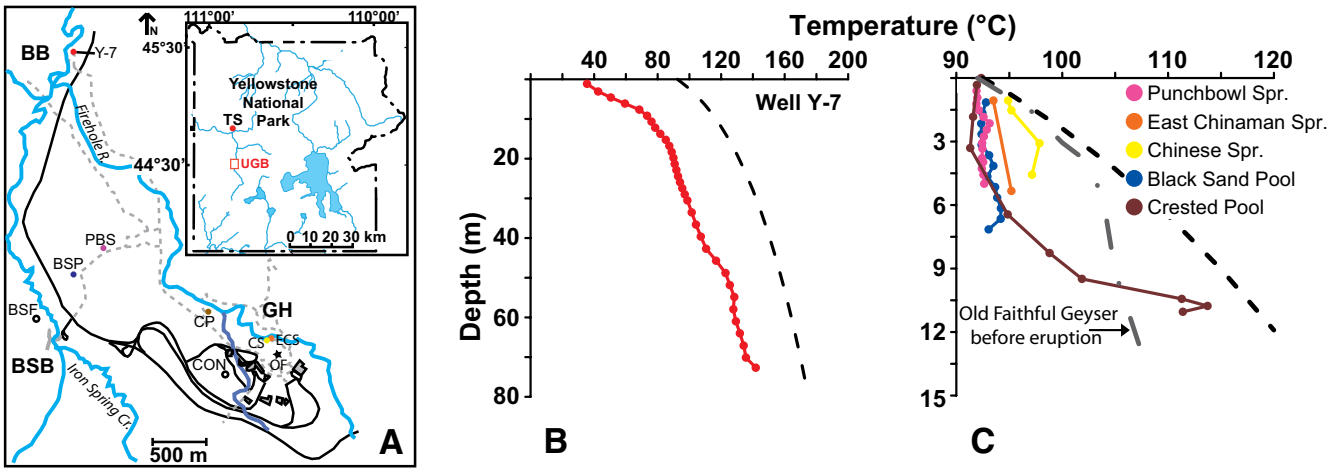

Figure 1. Map of Upper Geyser Basin (UGB) in Yellowstone National Park (Wyoming, USA). A: Locations of Biscuit Basin (BB), Black Sand Basin (BSB), Geyser Hill (GH), and sampled pools and well Y-7 (colored circles). Two open black circles are for fumaroles with gas compositions presented in Figure 2. Black star is Old Faithful Geyser (OF). PBS—Punchbowl Spring; BSP—Black Sand Pool; CP—Crested Pool; CS—Chinese Spring; ECS—East Chinaman Spring; BSF—Black Sand fumarole, CON—Conoco fumarole. Inset shows map of Yellowstone National Park with location of UGB; TS—Terrace Spring. B: Temperature-depth profile in well Y-7 and reference boiling curve for pure water (dashed line). C: Temperature-depth profiles in thermal pools, reference boiling curve for pure water (dashed line), and temperature in Old Faithful Geyser conduit 15 s before eruption (dash-dot gray curve); data from Birch and Kennedy (1972).

sampling intervals with an accuracy of ±0.5 °C. Depth determinations have an accuracy of ±0.3 m. Details about the sampling are provided in Figure DR1 in the Data Repository, and procedures for the chemical analysis of thermal water and dissolved gases are provided in references listed in Tables DR2 and DR3.

RESULTS

The measured temperature profiles in the pools (Fig. 1C) suggest that the thermal waters are at temperatures just below water vapor saturation for the corresponding depth and the barometric pressure measured during the five-day experiment. Water chemistry (Table DR2; Fig. DR2) is similar to that of other thermal waters from the basin with HCO_3^-/Cl^- (mass) ≥1.9 in the northwest (well Y-7, Punchbowl Spring, Black Sand Pool) and ≤1.1 in the southeast, suggesting more extensive CO_2 degassing in the southeast (Fournier, 1989; Hurwitz et al., 2012). The concentration of dissolved CO_2 (mainly derived from magma) (Lowenstern et al., 2015) in all samples is approximately an order of magnitude greater than that of N_2 (mainly from air-saturated meteoric water [ASW]), approximately two orders of magnitude greater than those of O_2, CH_4, and Ar, and orders of magnitude greater than those of other noble gases (Table 1; Table DR3). This is similar to the composition of gases emerging from most of Yellowstone's thermal features (Chiodini et al., 2012; Bergfeld et al., 2014; Lowenstern et al., 2015). Sample YNP15-01 from the upper parts of well Y-7 is likely contaminated with air, as indicated by high concentrations of air-derived gases (Table 1) and noble gas isotope ratios (Table DR3). Therefore, this sample was excluded from the analysis and figures.

Dissolved gas concentrations in Black Sand and Crested Pools, both having a large surface area, are significantly lower and the pH values are higher (8.7–9.2; Table DR2) compared with the other pools that have a smaller surface area, and dissolved gas concentrations are much lower than those in the deep parts of well Y-7. Dissolved gas compositions in Black Sand and Crested Pools plot close to the composition of ASW, and those in the samples from Y-7 and Punchbowl Spring plot close to a CO_2-rich component, similar to two fumaroles from the Upper Geyser Basin (Fig. 2).

In contrast to the degassed pools, well Y-7 has substantial amounts of dissolved gas. Assuming that spatial variations of dissolved gas at depth are small, the higher gas concentrations and the CO_2-rich composition in Y-7 suggest that in the shallow subsurface reservoir, evaporation and degassing are minimal. In pools, evaporative heat flux driven by the vapor-pressure difference between the pool and the atmosphere is a function of wind speed, the temperature difference across the water-air interface, and the surface area of the pool (Adams et al., 1990; Hurwitz et al., 2014). At low vapor pressures, a gas phase rich in low-solubility gases such as N_2 will form (Kennedy et al., 1988).

DISCUSSION AND CONCLUSIONS

From the measured concentrations of dissolved gases, we calculate the partial pressures of the individual gases (P_i) (Table 1) given by Henry's law:

$$P_i\ (P,T) = X_i \cdot K_{Hi}, \qquad (1)$$

where T is temperature, X_i is the molar gas concentration (mole fraction) and K_H is the Henry's law constant (MPa/mole fraction). A gas phase can exsolve when the total dissolved gas pressure ($P_T = \Sigma P_i$) plus the vapor pressure of steam (P^s) is larger than the sum of the hydrostatic (P_{hyd}) and atmospheric (P_{atm}) pressures. To determine the K_H values of the dissolved gases at the sampling temperatures, we used the following semi-empirical formulation (Harvey, 1996):

$$\ln K_H = \ln P^s + \frac{A}{T^*} + \frac{B(1-T^*)^{0.355}}{T^*} + C\exp(1-T^*)(T)^{-0.41}, \qquad (2)$$

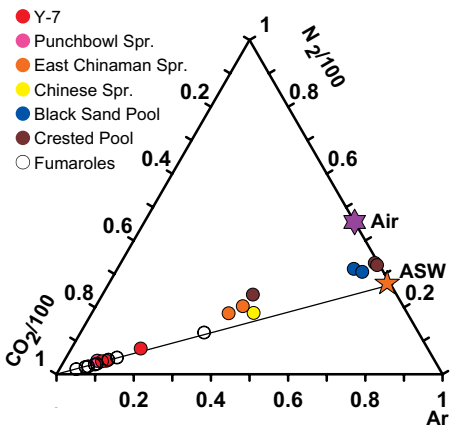

Figure 2. Composition of dissolved gases in thermal waters. Colored circles show composition of samples from thermal pools and from well Y-7 (Yellowstone, Wyoming, USA). Open black circles show compositions of two fumaroles in Upper Geyser Basin (Fig. 1). Data from Bergfeld et al. (2014). Air-saturated water (ASW; orange star) composition calculated from data of Wilhelm et al. (1977).

where $T^* = T/T_c$, and T_c is the critical temperature of water (647.14 K). The values of the coefficients A, B, and C for each dissolved gas are provided by Harvey (1996). Within the temperature range of interest, the calculated K_H values for CO_2 and N_2 are <2% different from those calculated using other formulations (Alvarez et al., 1988; Carroll et al., 1991). Salinity corrections to K_H are small (Barton and Chou, 1993) compared to the other errors associated with the determination of the partial pressure.

Because samples were collected at high temperatures while gas concentrations were determined at room temperature, we calculated the in-situ P_{CO_2} for the deep sample from well Y-7 (YNP15-03) using the chemical speciation code SOLMINEQ.88 (Kharaka et al., 1988). In these calculations, we used the CO_2 concentration and chemical composition of the sample measured in the laboratory (at 25 °C) and assumed that dissolved inorganic carbon and total alkalinity were conserved during cooling from in-situ temperatures. Results suggest that the difference in PCO_2 calculated with the speciation code and calculated from the measured CO_2 using Equation 1 is <12% (Table 1). Although CO_2 concentrations are mostly much higher than N_2 concentrations, when converted to partial pressures, $P_{N_2} > P_{CO_2}$, except for the two deep Y-7 samples (Table 1). The lower N_2 solubility relative to CO_2 at lower temperatures (Fig. DR3) is largely responsible for $P_{N_2} > P_{CO_2}$.

Using gas concentrations in sample YNP15-03 (70.1 m) from well Y-7 and the vapor saturation temperature of pure water at the local elevation (93 °C), temperature-depth (Z in meters) curves for $H_2O + CO_2$, $H_2O + N_2$, and $H_2O + CO_2$-N_2 vapor saturation were calculated:

$$Z = \frac{(P_{H_2O} + P_{CO_2} - P_{atm}) \cdot 1000}{\rho \cdot g}, \quad (3)$$

$$Z = \frac{(P_{H_2O} + P_{N_2} - P_{atm}) \cdot 1000}{\rho \cdot g}, \quad (4)$$

$$Z = \frac{(P_{H_2O} + P_{CO_2} + P_{N_2} - P_{atm}) \cdot 1000}{\rho \cdot g}, \quad (5)$$

where ρ is the average water density (958 kg/m^3 at 100 °C), g is the acceleration of gravity (9.81 m/sec^2), and P is pressure (kPa). We use the average ambient atmospheric pressure (P_{atm}) that was measured during the five-day experiment, 77.6 kPa. The contribution of other dissolved gases is within error, which we estimate at 10%, mainly resulting from analytical determinations and the range of solubility models.

Gas compositions from samples collected deeper in the pools plot close to the H_2O-CO_2-N_2, H_2O-CO_2, and H_2O-N_2 saturation curves and approach the H_2O saturation curve at shallower depths (Fig. 3). The three shallowest samples (<2 m) are also at temperatures above the H_2O-CO_2 saturation curve, suggesting progressive degassing at shallow levels in the pools. At greater depths, the two deep samples from well Y-7 (~51 m and 71 m) are at temperatures significantly below the vapor saturation temperature at the respective depths, implying minimal degassing.

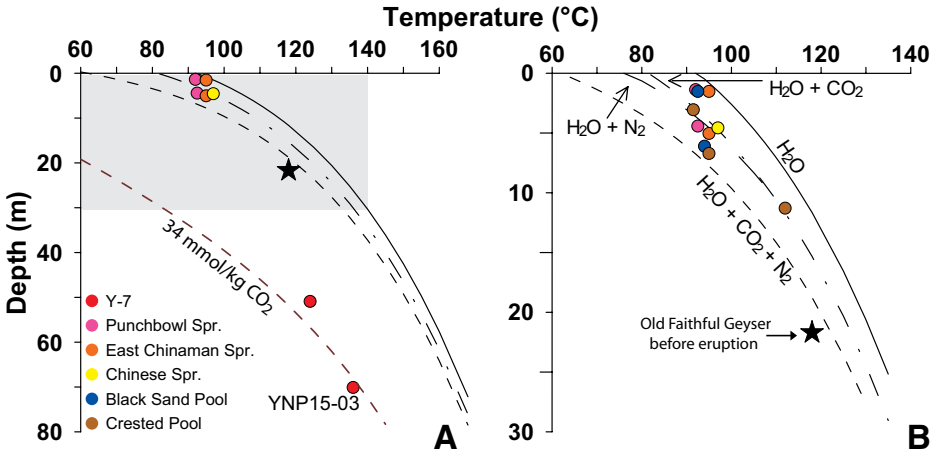

Figure 3. Temperature-depth curves. Saturation curves for H_2O-CO_2 (dash-dot curve), H_2O-N_2 (coarse-dashed curve) (only in B), and H_2O-CO_2-N_2 (fine-dashed curve) calculated with Equations 3, 4, and 5, respectively, and saturation curve for H_2O (solid curve) calculated using data from National Institute of Standards and Technology (http://webbook.nist.gov/chemistry/fluid/) database. Brown dashed curve is saturation curve representing recharge of 34 mmol/kg of CO_2 to sample YNP15-03. Temperature-depth of samples from pools and well Y-7 are in colored circles. Stars show maximum temperatures measured at depth of 21.7 in conduit of Old Faithful Geyser (Yellowstone National Park, Wyoming, USA) (Hutchinson et al., 1997). A: All samples plotted. Shaded rectangle shows temperature-depth range in B. B: Only samples from thermal pools are plotted. Sample YNP15-01 from upper parts of Y-7 is contaminated with air (Table 1) and not plotted.

Our measurements and calculations are consistent with a hypothesis based on temperature measurements in the conduit of Old Faithful Geyser (Fig. 1C) that "the observations to date suggest a significant presence of CO_2" and "any comparisons of P-T conditions in Old Faithful should be compared with a reference boiling curve for an H_2O-CO_2 mixture" (Hutchinson et al., 1997, p. 878). The hottest temperature consistently recorded in the geyser conduit at a depth of 21.7 m was 118 °C, similar to earlier measurements made in 1949 (Birch and Kennedy, 1972). This temperature is 14 °C lower than the vapor saturation temperature of pure water at that depth (Fig. 3). Below-boiling maximum temperatures were also measured in the conduit of the Great Geysir in Iceland (Birch and Kennedy, 1972). The maximum temperature in the Old Faithful conduit is slightly lower than the H_2O-CO_2-N_2 saturation temperature at 21.7 m, as calculated from the composition of sample YNP15-03 and Equation 5 (Fig. 3). The low measured temperature at the bottom of the conduit implies that bubbles formed in the Old Faithful Geyser reservoir ("bubble trap") (Vandemeulebrouck et al., 2013) probably contain H_2O-CO_2-N_2 mixtures. The relatively constant intervals of Old Faithful Geyser (Hurwitz et al., 2014) and Lone Star Geyser (~5 km south-southeast of Old Faithful Geyser) (Karlstrom et al., 2013) imply that heat and gas recharge into the reservoir is relatively constant.

The lethal hydrothermal eruption at Ontake-san in Japan in September 2014 (57 people were killed) was preceded by 10 yr of gas influx into the shallow subsurface reservoir (Sano et al., 2015). To quantify the effects of gas recharge into shallow hydrothermal reservoirs in Yellowstone, we assume a reservoir at the depth of sample YNP15-03 from well Y-7 (70.1 m, 136 °C). This depth is representative for source depths of hydrothermal eruptions in Yellowstone (61 ± 15 m), inferred from exposed glacial deposits and lake sediments (Muffler et al., 1971). We calculate that if 34 mmol/kg of CO_2 (10× the measured concentration in sample YNP15-03) or a multi-component gas mixture would be recharged into the reservoir, a two-phase fluid would form at that depth (Fig. 3). This additional CO_2 is twice the CO_2 concentration (but within analytical uncertainties) inferred for Terrace Spring (Fig. 1A) along the northern boundary of Yellowstone caldera (Lowenstern et al., 2005) and only slightly higher than the calculated concentration of the parent fluid in Heart Lake Geyser Basin at the southern margin of the Yellowstone caldera (21 mmol/L) (Lowenstern et al., 2012). The 34 mmol/kg of CO_2 can be injected into the shallow hydrothermal reservoirs within days, as inferred from the calculated CO_2 flux into the Ontake-san reservoir prior to its 2014 eruption (~80 mol/day of CO_2 over 10 yr) (Sano et al., 2015). Gas recharge into the shallow reservoir could result from seismic activity; for example, in Ontake-san, the eruption took place two and a half weeks

following seismicity levels significantly above background. In Yellowstone, seismic fluid-driven swarms in the shallow crust are common (Farrell et al., 2009; Shelly et al., 2013), and a large swarm in the eastern part of Yellowstone caldera in 1978 was followed by a spike in CO_2 discharge (Evans et al., 2010).

We suggest that monitoring changes in gas emission rate and composition in areas with neutral and alkaline chloride thermal waters could provide important information on the natural resources (geysers) and hazards (eruptions) in these areas. Such measurements would be especially important following large earthquakes and earthquake swarms.

ACKNOWLEDGMENTS

We thank David Roth and Jeff Cullen for help with field work, and the Research permit office at Yellowstone National Park for assistance with field planning and logistics. We thank Jake Lowenstern and three anonymous journal reviewers for comments and suggestions, and Cathy Ryan and Bethany Ladd for discussions. This study was funded by the U.S. Geological Survey Volcano Hazards Program.

REFERENCES CITED

Adams, E.E., Cosler, D.J., and Helfrich, K.R., 1990, Evaporation from heated water bodies: Predicting combined forced plus free convection: Water Resources Research, v. 26, p. 425–435, doi:10.1029/WR026i003p00425.

Alvarez, J., Crovetto, R., and Fernández-Prini, R., 1988, The dissolution of N_2 and of H_2 in water from room temperature to 640 K: Berichte der Bunsengesellschaft fur Physikalische Chemie, v. 92, p. 935–940, doi:10.1002/bbpc.198800223.

Barton, P.B., and Chou, I., 1993, Calculation of the vapor-saturated liquidus for the NaCl-CO_2-H_2O system: Geochimica et Cosmochimica Acta, v. 57, p. 2715–2723, doi:10.1016/0016-7037(93)90385-A.

Bergfeld, D., Lowenstern, J.B., Hunt, A.G., Shanks, W.C.P., III, and Evans, W.C., 2014, Gas and isotope chemistry of thermal features in Yellowstone National Park, Wyoming (version 1.1): U.S. Geological Survey Scientific Investigations Report 2011-5012, 28 p., with data files.

Birch, F., and Kennedy, G.C., 1972, Notes on geyser temperatures in Iceland and Yellowstone National Park, *in* Heard, H.C., et al., eds., Flow and Fracture of Rocks: American Geophysical Union Monograph 16, p. 329–336, doi:10.1029/GM016p0329.

Browne, P.R.L., and Lawless, J.V., 2001, Characteristics of hydrothermal eruptions, with examples from New Zealand and elsewhere: Earth-Science Reviews, v. 52, p. 299–331, doi:10.1016/S0012-8252(00)00030-1.

Carroll, J.J., Slupsky, J.D., and Mather, A.E., 1991, The solubility of carbon dioxide in water at low pressure: Journal of Physical and Chemical Reference Data, v. 20, p. 1201–1209, doi:10.1063/1.555900.

Chiodini, G., Caliro, S., Lowenstern, J.B., Evans, W.C., Bergfeld, D., Tassi, F., and Tedesco, D., 2012, Insights from fumarole gas geochemistry on the origin of hydrothermal fluids on the Yellowstone Plateau: Geochimica et Cosmochimica Acta, v. 89, p. 265–278, doi:10.1016/j.gca.2012.04.051.

Christiansen, R.L., Lowenstern, J.B., Smith, R.B., Heasler, H., Morgan, L.A., Nathenson, M., Mastin, L.G., Muffler, L.J.P., and Robinson, J.E., 2007, Preliminary assessment of volcanic and hydrothermal hazards in Yellowstone National Park and vicinity: U.S. Geological Survey Open-File Report 2007-1071, 94 p.

Evans, W.C., Bergfeld, D., McGeehin, J.P., King, J.C., and Heasler, H., 2010, Tree-ring ^{14}C links seismic swarm to CO_2 spike at Yellowstone, USA: Geology, v. 38, p. 1075–1078, doi:10.1130/G31345.1.

Farrell, J., Husen, S., and Smith, R.B., 2009, Earthquake swarm and *b*-value characterization of the Yellowstone volcano-tectonic system: Journal of Volcanology and Geothermal Research, v. 188, p. 260–276, doi:10.1016/j.jvolgeores.2009.08.008.

Fournier, R.O., 1989, Geochemistry and dynamics of the Yellowstone National Park hydrothermal system: Annual Review of Earth and Planetary Sciences, v. 17, p. 13–53, doi:10.1146/annurev.ea.17.050189.000305.

Harvey, A.H., 1996, Semiempirical correlation for Henry's constants over large temperature ranges: AIChE (American Institute of Chemical Engineers) Journal, v. 42, p. 1491–1494, doi:10.1002/aic.690420531.

Hurwitz, S., and Lowenstern, J.B., 2014, Dynamics of the Yellowstone hydrothermal system: Reviews of Geophysics, v. 52, p. 375–411, doi:10.1002/2014RG000452.

Hurwitz, S., Hunt, A.G., and Evans, W.C., 2012, Temporal variations of geyser water chemistry in the Upper Geyser Basin, Yellowstone National Park, USA: Geochemistry Geophysics Geosystems, v. 13, Q12005, doi:10.1029/2012GC004388.

Hurwitz, S., Sohn, R.A., Luttrell, K., and Manga, M., 2014, Triggering and modulation of geyser eruptions in Yellowstone National Park by earthquakes, earth tides, and weather: Journal of Geophysical Research, v. 119, p. 1718–1737, doi:10.1002/2013JB010803.

Hutchinson, R.A., Westphal, J.A., and Kieffer, S.W., 1997, In situ observations of Old Faithful Geyser: Geology, v. 25, p. 875–878, doi:10.1130/0091-7613(1997)025<0875:ISOOOF>2.3.CO;2.

Karlstrom, L., Hurwitz, S., Sohn, R., Vandemeulebrouck, J., Murphy, F., Rudolph, M.L., Johnston, M.J.S., Manga, M., and McCleskey, R.B., 2013, Eruptions at Lone Star Geyser, Yellowstone National Park, USA: 1. Energetics and eruption dynamics: Journal of Geophysical Research, v. 118, doi:10.1002/jgrb.50251.

Kennedy, B.M., Reynolds, J.H., and Smith, S.P., 1988, Noble gas geochemistry in thermal springs: Geochimica et Cosmochimica Acta, v. 52, p. 1919–1928, doi:10.1016/0016-7037(88)90015-4.

Kharaka, Y., Gunter, W.D., Aggarwal, P.K., Perkins, E.H., and DeBraal, J.D., 1988, SOLMINEQ.88: A computer program for geochemical modeling of water-rock interactions: U.S. Geological Survey Water Resources Investigation Report 88-4227, 420 p.

Kieffer, S.W., 1989, Geologic nozzles: Reviews of Geophysics, v. 27, p. 3–38, doi:10.1029/RG027i001p00003.

Ladd, B., 2014, Insights into geyser behavior: The role of non-condensable gas [M.S. thesis]: Calgary, University of Calgary, 101 p.

Lowenstern, J.B., Evans, W.C., and Bergfeld, D., 2005, Diffuse and direct sources of CO_2 from Terrace Springs, a large-discharge travertine-forming spring at Yellowstone National Park, *in* Proceedings, 9th Workshop of the International Association of Volcanology and Chemistry of the Earth's Interior Commission on the Chemistry of Volcanic Gases, Palermo, Sicily.

Lowenstern, J.B., Bergfeld, D., Evans, W.C., and Hurwitz, S., 2012, Generation and evolution of hydrothermal fluids at Yellowstone: Insights from the Heart Lake Geyser Basin: Geochemistry Geophysics Geosystems, v. 13, Q01017, doi:10.1029/2011GC003835.

Lowenstern, J.B., Bergfeld, D., Evans, W.C., and Hunt, A.G., 2015, Origins of geothermal gases at Yellowstone: Journal of Volcanology and Geothermal Research, v. 302, p. 87–101, doi:10.1016/j.jvolgeores.2015.06.010.

Lu, X., and Kieffer, S.W., 2009, Thermodynamics and mass transport in multicomponent, multiphase H_2O systems of planetary interest: Annual Review of Earth and Planetary Sciences, v. 37, p. 449–477, doi:10.1146/annurev.earth.031208.100109.

Mastin, L.G., 1995, Thermodynamics of gas and steam-blast eruptions: Bulletin of Volcanology, v. 57, p. 85–98, doi:10.1007/BF00301399.

Morgan, L.A., Shanks, W.C.P., III, and Pierce, K.L., 2009, Hydrothermal Processes above the Yellowstone Magma Chamber: Large Hydrothermal Systems and Large Hydrothermal Explosions: Geological Society of America Special Paper 459, 95 p., doi:10.1130/2009.2459(01).

Muffler, L.P., White, D.E., and Truesdell, A.H., 1971, Hydrothermal explosion craters in Yellowstone National Park: Geological Society of America Bulletin, v. 82, p. 723–740, doi:10.1130/0016-7606(1971)82[723:HECIYN]2.0.CO;2.

Sano, Y., Kagoshima, T., Takahata, N., Nishio, Y., Roulleau, E., Pinti, D.L., and Fischer, T.P., 2015, Ten-year helium anomaly prior to the 2014 Mt Ontake eruption: Scientific Reports, v. 5, 13069, doi:10.1038/srep13069.

Shelly, D.R., Hill, D.P., Massin, F., Farrell, J., Smith, R.B., and Taira, T., 2013, A fluid-driven earthquake swarm on the margin of the Yellowstone caldera: Journal of Geophysical Research, v. 118, p. 4872–4886, doi:10.1002/jgrb.50362.

Thiéry, R., and Mercury, L., 2009, Explosive properties of water in volcanic and hydrothermal systems: Journal of Geophysical Research, v. 114, B05205, doi:10.1029/2008JB005742.

Vandemeulebrouck, J., Roux, P., and Cros, E., 2013, The plumbing of Old Faithful Geyser revealed by hydrothermal tremor: Geophysical Research Letters, v. 40, p. 1989–1993, doi:10.1002/grl.50422.

White, D.E., 1967, Some principles of geyser activity, mainly from Steamboat Springs, Nevada: American Journal of Science, v. 265, p. 641–684, doi:10.2475/ajs.265.8.641.

White, D.E., Fournier, R.O., Muffler, L.J.P., and Truesdell, A.H., 1975, Physical results of research drilling in thermal areas of Yellowstone National Park, Wyoming: U.S. Geological Survey Professional Paper 892, 70 p.

Wilhelm, E., Battino, R., and Wilcock, R.J., 1977, Low-pressure solubility of gases in liquid water: Chemical Reviews, v. 77, p. 219–262, doi:10.1021/cr60306a003.

Manuscript received 30 October 2015
Revised manuscript received 25 January 2016
Manuscript accepted 29 January 2016

Printed in USA